Chapter 4

PHOTOPHYSICS

One only has to attempt the synthesis of **1** to truly appreciate the fluorescence properties of the molecule. On a column that is completely black with products, a single band shines brightly under long-wavelength UV light, identifying the corrole. A question that immediately comes to mind when observing this concerns the quantification of these properties.

Work on photophysics focused mainly on the excited singlet state of the corroles, though some work on characterization of the excited triplet state will be presented at the end of this chapter.

Singlet Emission and the Four-Orbital Model

Looking first at the metallocorrole complexes, the effects predicted by the four-orbital model can again be seen (see table 4.1). The fluorescence of the complexes with the more electropositive gallium(III) show a red-shift in comparison to their counterparts with the less electropositive tin(IV) centers. And, as with the absorption spectra, a red-shift is also seen when keeping the metal identity the same and changing the identity of the β substituents from hydrogen to sulfonate groups (see figures 4.1, 4.2). It can also be seen that each of the corrole emission spectra has a vibronic band 1300-1400 cm^{-1} to the red of each peak.

Compound	Emission Peak (nm)
1	648
2 (pH 7)	632
2 (pH 2)	628, 664
1-Ga	607
2-Ga	629
1-Sn	605
2-Sn	615

Table 4.1. Peak positions for singlet emission of the corroles used in this study.

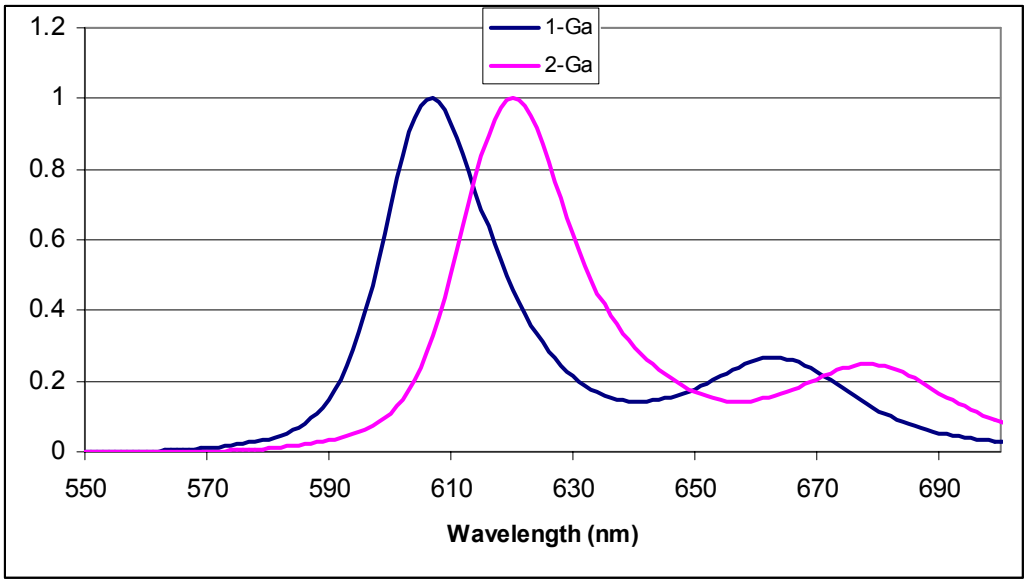

Figure 4.1. Singlet emission spectra for **1-Ga** (blue, in toluene) and **2-Ga** (pink, in pH 7.0 buffer). Peak intensity is normalized to 1 (arbitrary units).

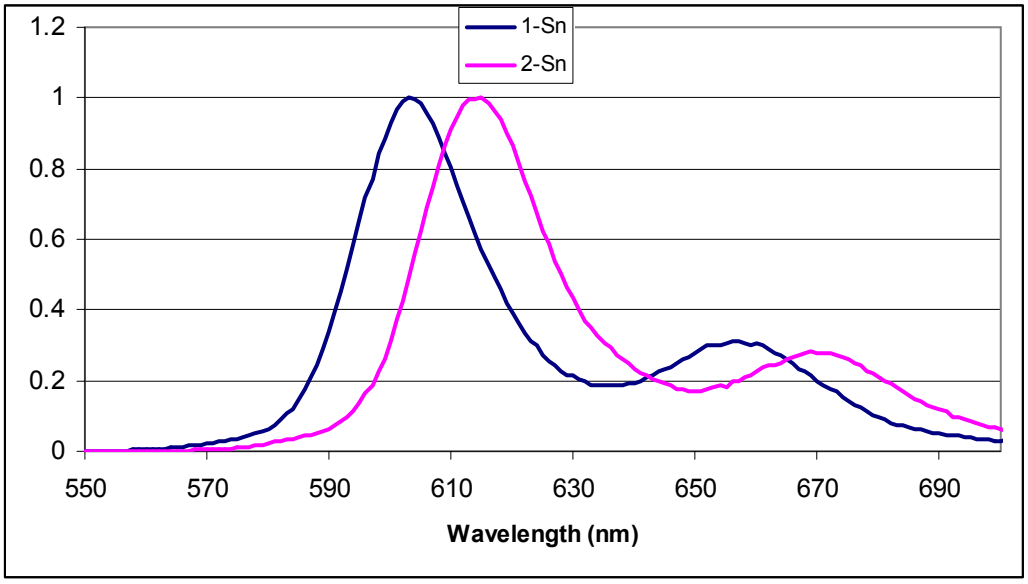

Figure 4.2. Singlet emission spectra for **1-Sn** (blue, in toluene) and **2-Sn** (pink, in pH 7.0 buffer). Peak intensity is normalized to 1 (arbitrary units).

On first glance, it would appear that the situation is very different for the two metal-free corroles (see figure 4.3). In this pair, it is the emission of the nonsulfonated corrole that is significantly red-shifted in comparison to the sulfonated. While this could appear to be a demonstration of the unpredictable effects of β substitution, closer inspection reveals the difference lies in the nature of the emitting species. While all the other corroles studied here show a 10-20 nm difference between the emission peak and the lowest energy Q-band peak, the difference in **1** is 46 nm. This difference can be explained by the protonation state of the molecule. The spectrum of **2** was measured in pH 7.0 buffer. However, as seen in chapter 2, at this pH one of the core protons of **2** has been lost, reducing the steric strain on the molecule, and this spectrum is really the singlet emission of $\mathbf{2}^-$. Note that the spectrum of **1** was measured in toluene, which would not give it the same opportunity for deprotonation as **2**. Thus, to gauge the effect of the sulfonate groups for these molecules, a comparison must be made between **1** and **2** at an intermediate pH where **2** will be core neutral, such as pH 3.8 (see figure 4.4). From these spectra, it can be easily seen that the effect of the sulfonate groups does indeed hold for the free-base corroles, and a red-shift is observed between like species. It is also expected that if **1** were to be deprotonated to $\mathbf{1}^-$, the fluorescence spectrum would blue-shift 25-35 nm.

An interesting effect is seen upon further protonation of **2**, as seen in figure 4.5. The emission spectrum for $\mathbf{2}^+$ shows a peak slightly blue-shifted compared to the peak of $\mathbf{2}^-$. If steric distortion is responsible for the large red-shift observed in going from $\mathbf{2}^-$ to **2**, these data would suggest that the distortion is counterbalanced when a fourth proton is added to the corrole macrocycle. This can be explained by the fourth proton adding to the opposite

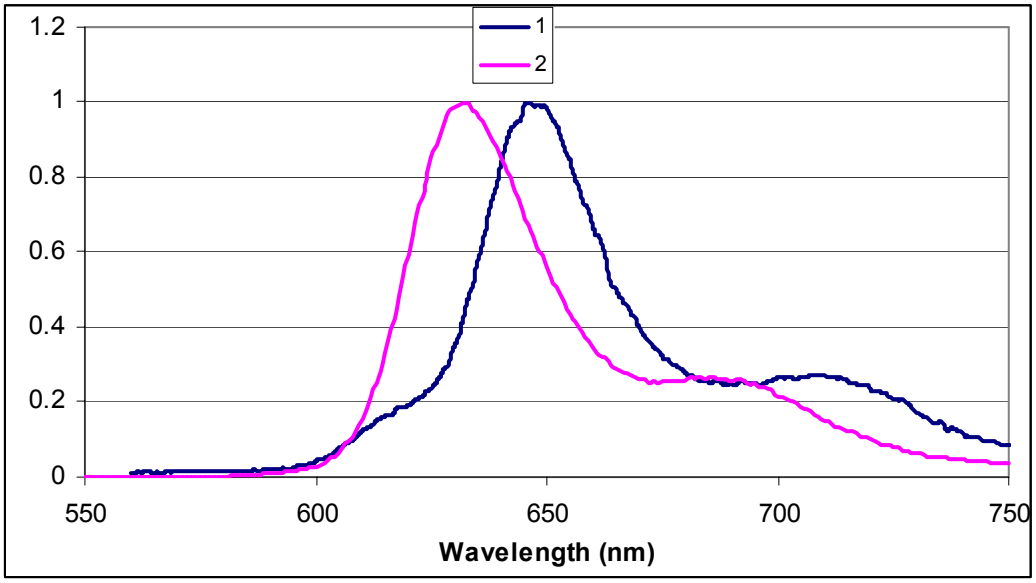

Figure 4.3. Singlet emission spectra for **1** (blue, in toluene) and **2** (pink, in pH 7.0 buffer). Peak intensity is normalized to 1 (arbitrary units).

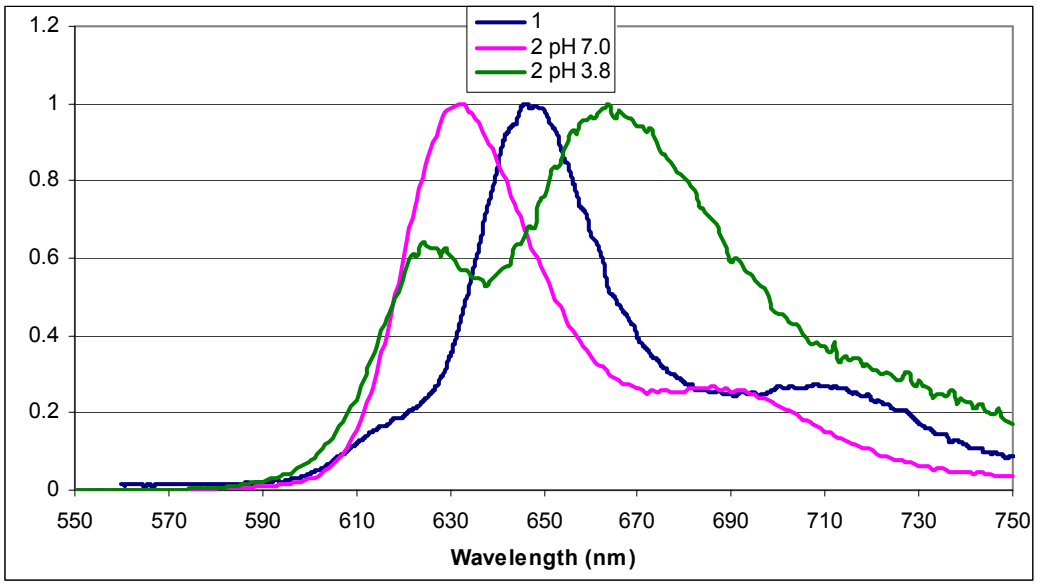

Figure 4.4. Singlet emission spectra of **1** (blue, in toluene), $\mathbf{2}^-$ (pink, in pH 7.0 buffer), and **2** (green, in pH 3.8 buffer). Peak intensities have been normalized to 1 (arbitrary units).

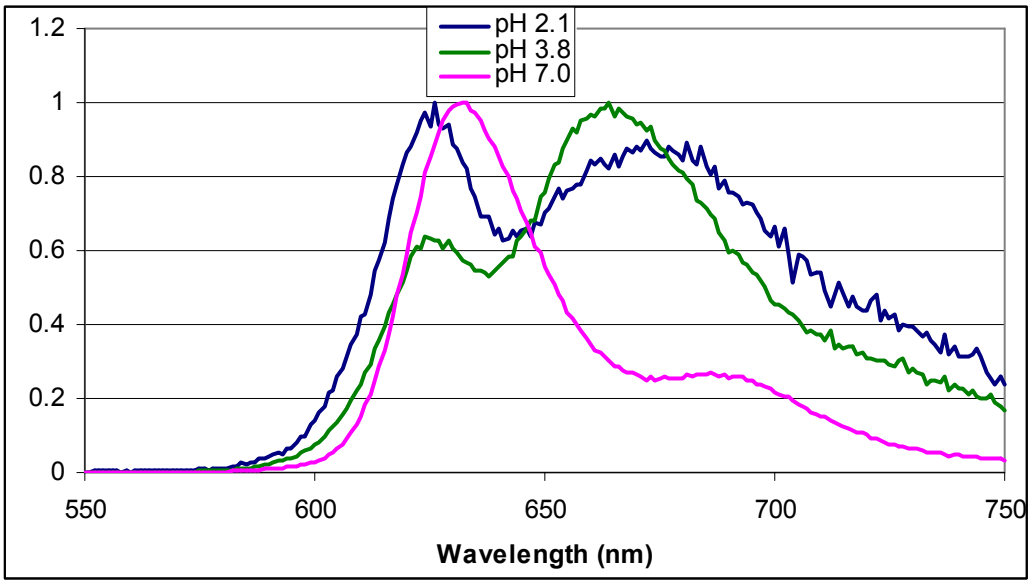

Figure 4.5. Emission spectra of $\mathbf{2}^-$ (pink, in pH 7.0 buffer), **2** (green, in pH 3.8 buffer), and $\mathbf{2}^+$ (blue, in pH 2.1 buffer). Peak intensities have been normalized to 1 (arbitrary units). Note there is some contamination of $\mathbf{2}^+$ in the spectrum of **2** and vice versa.

side of the corrole than the previous proton, forcing the macrocycle to distort back toward planarity. An idealized case is shown in figure 4.6. It is important to note that while the pyrrole rings in the figure are all shown as being perfectly planar, this is not likely to be the case. However, the rings are likely closer to being in the mean plane of the four nitrogens of $\mathbf{2}^{+}$ than in the case of **2**.

Singlet Lifetimes

This part of the project also investigated lifetimes of corrole singlet excited states by monitoring emission with a picosecond laser and streak camera set up. The data for **1** are shown in figure 4.7, along with the lifetime fit. As seen in the figure, the lifetime of **1** can be calculated to be 5 nanoseconds. The figure also illustrates a problem encountered in the measurement of these lifetimes, namely multiple decay times. The data for **1** show ~25% decaying with a lifetime of 1 nanosecond. It is thought that this is due to oxygen quenching. While care was taken to degas the solution (three freeze-pump-thaw cycles), the lifetimes (and as will be seen shortly, the quantum yields) show great sensitivity to the presence of any oxygen. While this makes absolute determination of the lifetimes difficult, they can still be estimated, albeit with proportionally large error bars. All six of the fluorescent corroles tested herein were found to have singlet lifetimes of 5 ± 3 ns.

Singlet Quantum Yields

The final characterization of the singlet excited state was measurement of the quantum yields. Much like the lifetimes, the quantum yield measurements suffered from

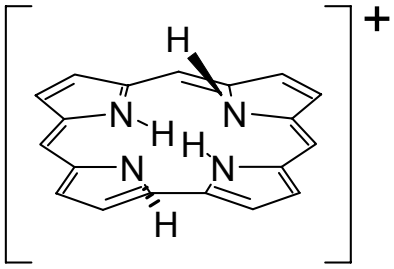

Figure 4.6. An idealized planar structure of $\mathbf{2}^{+}$. Note that while the pyrrole rings are shown as being in the mean plane of the four nitrogens, this is not likely to be the actual case. See text for further discussion.

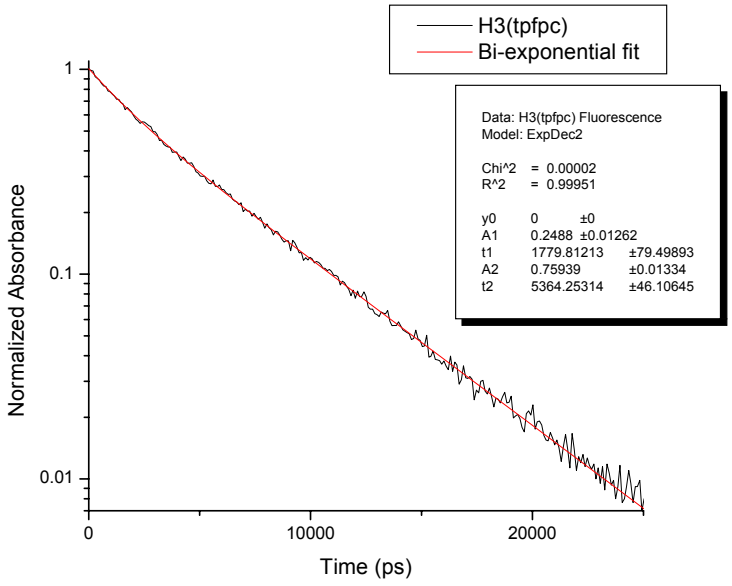

Figure 4.7. Fluorescence emission decay (black) and fit (red) for **1**.

reproducibility problems. Through variations in the concentration of the solutions used, the standard used, and the methods used to prepare the solutions, yields varying by a full order of magnitude were obtained. Reported here are best values based on a number of experiments on degassed solutions in which care was taken to avoid aggregation effects, and with a standard that has been very well studied in the group, ruthenium trisbipyridine.

The general set-up used for measuring quantum yields involved the preparation of solutions of the compounds at low concentrations. For the particular fluorimeter used for these experiments, overall absorbance at the excitation wavelength needed to be below 0.1 absorbance units to ensure linearity of response. In general, the solutions used herein were kept at absorbances below 0.05 units. A solution containing ruthenium trisbipyridine was also made to the same specifications. All solutions were made to have approximately the same absorbance at the excitation wavelength for a given set of experiments. The solutions were degassed by three freeze-pump-thaw cycles in atmosphere controlled cuvettes, and the emission spectra were measured. The quantum yields were then calculated from the following equations[22]:

$$\Phi_f = \Phi_{ref}\left(\frac{n^2}{n_{ref}^2}\right)\left(\frac{\int F(\nu)d\nu}{A}\right)\left(\frac{A_{ref}}{\int F_{ref}(\nu)d\nu}\right) \qquad \text{(eq. 4.1)}$$

$$F(\nu) = F(\lambda)\lambda^2 \qquad \text{(eq. 4.2)}$$

In eq. 4.1, Φ is the quantum yield (0.042 for $Ru(bpy)_3$), *n* is the refractive index of the solvent, ∫F(ν)dν is the area under the curve of fluorescence intensity vs. wavenumber, and

A is the absorbance at the excitation wavelength (430 nm for these experiments). Unsubscripted quantities are those of the sample; quantities subscripted "ref" are for the reference solution. Since the fluorescence spectra were measured versus wavelength, equation 4.2 was used to convert the intensities to a function of wavenumber. Due to the various solubilities of the corroles, no one solvent could be used for all six, so several solvents were used. Table 4.2 presents the average results from these experiments. Given the spread of values obtained, the errors in these numbers are estimated to be ± 15%.

As can be seen in the table, the free-base and gallium corroles all possess quantum yields of 10% or higher, while the tin complexes are roughly an order of magnitude lower, as expected, given that the heavy atom effect should come into play for the tin corroles, promoting intersystem crossing to the triplet state.

Triplet States

An attempt was also made to detect the presence of this triplet state for four metallocorroles through the use of transient absorbance, thereby giving lifetime information as well. The triplet lifetime of **1** had previously been measured at 870 μs[8]. The metallocorrole solutions were observed at 850 nm, beyond the presence of any intensity from fluorescence. In all four cases, a long-lived excited state was observed, and like the singlet observations, the decay was biexponential, with ~80% of the sample decaying with the shorter lifetime. These lifetimes are given in table 4.3. The biexponential nature of the decays again gives evidence of the sensitivity of these compounds to oxygen and concentration effects. While the solutions were made in as low a concentration as feasible

Compound	Φ_f
1	0.10
2 (pH 7.0)	0.18
2 (pH 2.1)	0.03
1-Ga	0.16
2-Ga	0.15
1-Sn	0.01
2-Sn	0.03

Table 4.2. Quantum yields for fluorescence of corroles in this study. **1, 1-Ga, 1-Sn** were measured in toluene, **2** in buffer at given pHs, **2-Ga** in methanol, and **2-Sn** in isopropanol. Error is estimated at 15%.

	τ_1 (μs)	τ_2 (ms)
1-Ga	110	0.45
2-Ga	730	2.0
1-Sn	100	1.0
2-Sn	120	1.2

Table 4.3. Excited triplet lifetimes for four metallocorroles.

to still obtain a measurable transient absorbance signal, it is possible that even at this concentration there was some corrole aggregation. No aggregation effects were seen in this concentration range by absorbance, however. Given the previously measured lifetime of **1**, it seems reasonable that the triplet state could decay with the shorter lifetimes measured, as the heavy atom effect would be expected to shorten this value compared to the free-base.

Conclusions

The relative positions of the singlet emission bands of the corroles provide further support for the four-orbital model discussed in chapter 3. As well, it has been seen that the position of the singlet emission bands for the free-bases can be used to determine the protonation state of the molecule, or at the least, give an estimate of the planarity.

While the excited states of these compounds show great sensitivity toward concentration and oxygen, their quantum yields and lifetimes can be estimated. Interestingly, the quantum yields measured for the free-bases and gallium complexes (10 and 18% for the free-bases, 15 and 16% for the gallium corroles) are much higher than their porphyrin counterparts. Tetrakis(pentafluorophenyl)porphyrin has a measured quantum yield of 3.2%[23], and the zinc complex has a measured quantum yield of 7%[24]. It is believed that the greater quantum yields for the corroles are properties related to the direct pyrrole-pyrrole linkage, as this structural element makes the macrocycle more rigid, thereby disfavoring relaxation to the ground state through ring bending and stretching. This effect is also manifested in the lifetimes of porphyrins, as evidenced by the much shorter singlet lifetime (<1.0 ns) of zinc tetrakis(pentafluorophenyl)porphyrin[24].